

## ISEC 2005-76251

**AN ADAPTIVE PERTURB AND OBSERVE MAXIMUM POWER POINT TRACKING  
SYSTEM FOR PHOTOVOLTAIC ARRAYS**

Mohammad Serhan, Sami H. Karaki, and Lana R. Chaar

*Department of Electrical and Computer Engineering  
American University of Beirut  
P.O. Box: 11 0236, Beirut, Lebanon 1107 2020***ABSTRACT**

This paper presents a maximum power point (MPP) hardware tracking system based on an adaptive Perturb and Observe (PAO) algorithm. Under a given solar and temperature condition the search for the MPP starts with a large perturbation step. When a drop in the delivered power is detected, the size of the step is halved and the direction of duty cycle change is reversed. Eventually the MPP will be tracked by small perturbation step (e.g. 1/ 255). When tracking at a maximum and a sudden change occurs in the atmospheric conditions, the system will try to reach the new MPP, with an adaptive perturbation step size that is allowed to increase after 4 consecutive increases or decrease in the duty cycle leading to increase in power delivery. This adaptive PAO algorithm forces the system to respond fairly quickly to any changes in the solar radiation or temperature level irrespective of where the previous operating point MPP was and without deteriorating the tracking efficiency. A tracking efficiency of about 96% was achieved using a very simple controller.

**Keywords:** Solar energy, Power Electronics, PV cells, Battery charging

**INTRODUCTION**

Energy is fundamental to the wellbeing of our society; it powers our homes, businesses, industries, and our life in general. However, energy, obtained from fossil fuels is now presenting global challenges; not only these energy resources are depletable but are also major contributors to atmospheric pollution and global warming. Renewable Energy is a new trend in clean energy production, which includes power generated from water, wind, solar radiation, biomass and other resources. This development of renewable power sources will save fossil fuel resources, and help improve the quality of the environment. One of the prominent renewable energy sources is electric energy from the sun through photovoltaic (PV) arrays,

which has a great potential because it makes use of the most abundant energy on earth.

A PV array has a current-voltage characteristic curve with a maximum power point (MPP) that varies with changing atmospheric conditions, i.e. solar radiation and temperature. An important consideration in the design of an efficient PV system is to track the MPP correctly as the temperature and solar radiation vary. This problem has received a good deal of attention by researchers in their effort to build efficient PV systems. Hussein et al [1] claim that the Incremental Conductance (IC) technique is better than that of Perturb and Observe (PAO) under rapidly changing atmospheric conditions. He tested both algorithms and reported that the efficiency of the power extracted from a PV array using the IC algorithm (89.9%) is higher than that of the PAO algorithm (81.5%). Koutroulis et al [2] compare between different algorithms to track the MPP of a PV array. Then he presents a new tracking scheme, based on the PAO method that uses the dc/dc converter duty cycle as a control parameter and forces the rate of change of power with respect to duty cycle change to zero. His experimental results showed a 15% increase in the PV output power as compared to the case where the dc/dc converter duty cycle is set such that the PV array produces maximum power at an irradiation level of 1000 W/m<sup>2</sup> at 25 °C. Yu et al [4] combine two existing algorithms, the constant voltage control and the IC method to track the MPP. Experimental results show that the proposed two-mode MPPT control improves the efficiency of the power generation and show excellent results at less than 30% insolation intensity. Masoum et al [5] present two simple maximum power-point tracking techniques known as voltage-based MPPT and current-based MPPT, which say that the voltage, or current, at the MPP is given as the product of the open-circuit voltage, or short-circuit current, times some factor. A procedure for determining the voltage or current factor is given in the paper. The voltage-based method is reportedly more efficient with less circuit losses. A reference

voltage method is implemented by Sweigers and Enslin [6, 7] in which the maximum power point tracker algorithm samples the open circuit voltage of the PV panel regularly by switching the converter off. The reference voltage is determined as a fixed percentage (e.g. 76%) of the open-circuit voltage; if the controller detects a panel voltage higher than the reference voltage, the duty cycle is increased causing an increase in the current and a decrease in the panel operating voltage. If the panel's voltage is lower than the reference voltage, the duty cycle is decreased. Hohm and Ropp [8] provide a comprehensive experimental comparison between different MPPT algorithms. After presenting the advantages and disadvantages of each algorithm, an experiment on the same setup PV array is run. Results show that the IC method has the highest efficiency (98%) in terms of power extracted from the PV array, next is the PAO technique efficiency (96.5%), and finally the reference voltage method efficiency (88%). However the complexity of the IC algorithm and the increased cost of its circuitry, encourage all to implement the PAO technique.

In this paper, a MPP tracking hardware system is designed and tested using an adaptive PAO algorithm. The PAO algorithm is enhanced by making the size of the perturbation adaptive to the conditions of the search for the MPP. Under a given solar and temperature condition the search for the MPP starts with a large perturbation step. As the power delivered increases with the duty cycle the size of the step is kept constant. Once a drop in the delivered power is detected, the size of the step is halved and the direction of duty cycle change is reversed. Eventually the MPP will be tracked by small perturbation depending on the hardware characteristics (e.g. 1/255). When tracking at a maximum and a sudden change occurs in the atmospheric conditions, the system will try to reach the new MPP, however with a very small perturbation step size. In such a case, and after 4 consecutive increases or decreases in the duty cycle leading to increase in power delivery, the perturbation size is doubled in order to overcome the loss in the solar power tracking efficiency associated with a rapidly varying weather conditions. This adaptive PAO algorithm forces the system to respond fairly quickly to any changes in the insolation or temperature level irrespective of where the previous operating point MPP was and without deteriorating the tracking efficiency. A tracking efficiency of about 96% was achieved using a very simple controller.

## MPPT SYSTEM HARDWARE

The system consists of a PV module, an H-bridge transformer-coupled converter, a 12V lead acid battery, and a control circuit that uses the PIC16F874 microcontroller as shown in Figure 1. The microcontroller samples the average current ( $I_s$ ) and voltage ( $V_s$ ) of the PV array, which vary depending on weather conditions temperature, and solar radiation. The sampled values are conditioned by a circuit interface, and fed through the analog to digital (A/D) ports of the microcontroller, which calculates the present power level and compares it with the previous one; if it is smaller then the

duty cycle is increased and if it is larger the duty cycle is reduced. The duty cycle change, or pulse width modulation (PWM), is performed through a special PWM built-in register. In this manner the system tracks the duty cycle at which the converter loads the PV module at the maximum power point (MPP) when charging the battery. The battery's state of charge is also controlled by the microcontroller to protect the battery from being overcharged, which behaves as a load that absorbs any available current provided by the converter during charging.

## Converter Control Circuit

The converter control circuit, shown in Figure 2 in block diagram, is based on an H-bridge configuration that employs electronic switches driven by square wave signals operating at 50% duty cycle. This permits good operation at high frequencies, avoiding problems that may arise when using variable duty cycle switching regulator. The control of the bridge output voltage ( $V_1 - V_2$ ) of this converter depends on controlling the phase difference between the voltages  $V_1$  and  $V_2$  as shown in Figure 3. This phase difference between  $V_1$  and  $V_2$  is generated by a phase splitter circuit and is equal to the width of the pulses generated by the PWM output of the microcontroller.

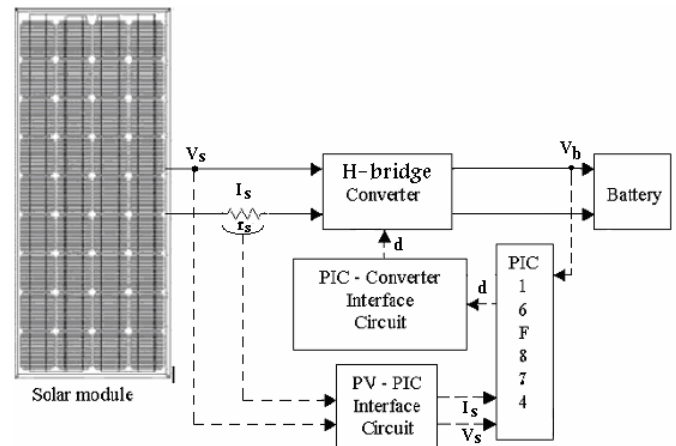


Figure 1: MPPT hardware system

The two output signals, square signal A and square signal B, will control the switching scheme of the four MOSFET switches  $T_1$ ,  $T_2$ ,  $T_3$ , and  $T_4$  of the H-bridge.  $T_1$  and  $T_2$  form a switch pair that controls the value of voltage  $V_1$  and are driven by the driver circuit 'A'.  $T_3$  and  $T_4$  switch pair similarly controls the value of voltage  $V_2$ , and are driven by the driver circuit 'B'. Switches  $T_1$  and  $T_2$  are operated by driver circuit 'A' using anti-phase driving signals: when  $T_1$  is closed,  $T_2$  is open and vice versa. The anti-phase signals also provide a dead-time interval during the transitions to permit the complete turn OFF of the switch (that was ON), before turning ON the other switch; this is necessary to avoid short-circuiting the battery and the flow of excessive currents in the transition interval. The operation of the driver circuit B is similar to that of driver circuit A.

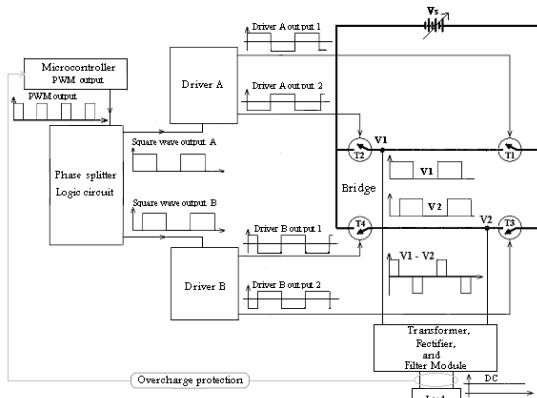


Figure 2. Converter and Controller

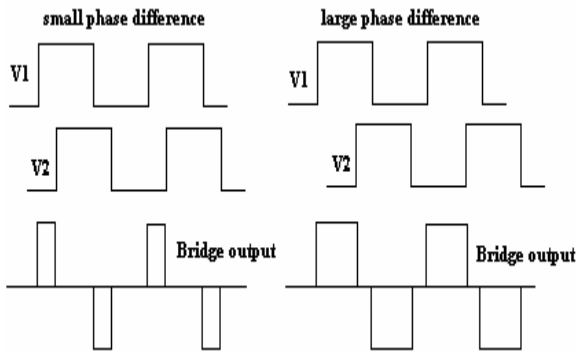


Figure 3. Bridge output with small and large phase difference

### Driver Circuit

The driver control circuit capable of providing the anti-phase signals to the gates of transistors  $T_1$  and  $T_2$  is shown in Figure 4. It provides the driving pulses with an amplitude of 12 V and a dead-time transition interval to ensure the complete turn ON of the switch that should be in the active mode (to have a low ON state resistance), and a fast turn OFF of the switch that should be deactivated. The comparators are used to convert the 5 volts logic levels (microcontroller output) to the 12 volts levels used to drive the gates of the MOSFETs. The 1 k $\Omega$  and the 1nF capacitors are used to delay the turn ON of each transistor, for an interval sufficient to make sure that the other transistor reaches the OFF state. Quick turn OFF is achieved by rapidly discharging the gate capacitance, and the 1nF capacitor, using diodes  $D_1$  and  $D_2$  that provide low resistance path for discharging current. Figure 9 shows details of the gate signals in which the clearance interval (dead time) is labeled by  $T_d$ . The MOSFET will not turn ON until the voltage between the gate and source reaches a threshold value ( $V_t$ ) of about 3 volts.

### The H-Bridge Circuit

As explained above Switches  $T_1$  and  $T_2$  are driven by anti-phase signals generated by driver circuit A. Similarly switches  $T_3$  and  $T_4$  are driven by anti-phase signals generated by the driver circuit B. These switches are n-channel enhanced mode power MOSFETs IRFZ46 as shown in Figure 5.

The power MOSFET IRFZ46, used for its high speed-switching capabilities, is a device rated at 50V and 50A, which means that the rating is well above maximum operating voltage and current which are 20 V and 6 A of the converter. It has a maximum leakage current of only 100 nA and a very low on-state resistance of 0.024 $\Omega$  and hence small conduction loss that makes it a highly efficient switching device.

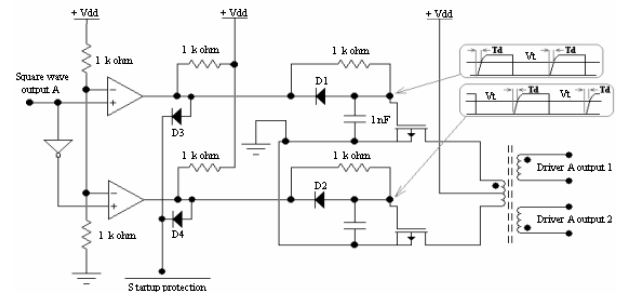


Figure 4. Driver 'A' schematic diagram

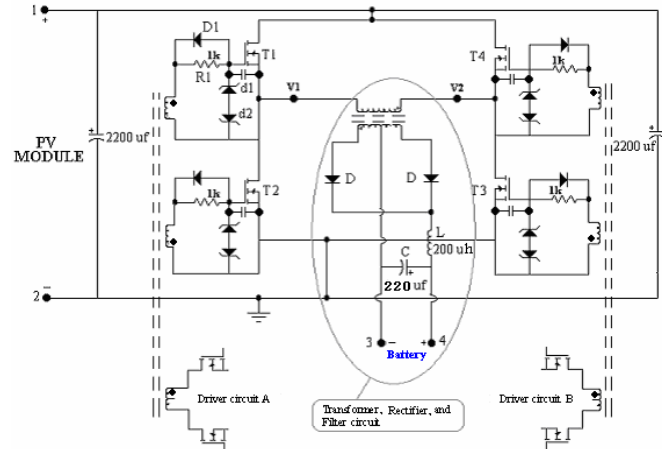


Figure 5. Bridge Converter schematic diagram

Although not shown in the figure, each transistor is equipped with a built-in fast-recovery power diode that provides a path for free-wheeling currents that flow during certain phases of operation. The transformer used here has a voltage transformation ratio of 1:1.5. Fast recovery diodes are used to rectify the bridge output by providing a unidirectional voltage, which is then filtered to produce a DC output equal to the average value of the pulse train. The elements of the rectifier and filter were chosen to keep the voltage and current ripple within specified bounds as explained below when the PV array is operating at its theoretical MPP of 70W.

**Inductor:** The inductance value is calculated by considering the case when the PV array operates at its maximum capacity (70 Watts). Therefore the output current can be calculated by using the equation  $P_{out} = V_o I_o$  where  $V_o$  is the battery voltage. Hence,  $I_o = P_o / V_o = 70 / 12 = 5.8$  A. The amplitude of the inductor current ripple is chosen to be at 10% of its dc value or 0.58A. The converter is selected to operate at

a frequency of 40 kHz obtained from a crystal oscillator running at 10 MHz and feeding an 8-bit register. The switching devices would allow easily an operation at 80 kHz that could be obtained from a 20 MHz crystal oscillator, but the choice was made based on availability. The value of the inductance is given by the following equation [9]:

$$L = \frac{V_0}{\Delta I_L} (1-D)T \quad (1)$$

where  $D$  is the duty cycle and  $T_s$  is the period of the PWM signal. The duty cycle is selected as  $D = V_o / V_d = 12 / 18 = 0.65$ . Thus the inductance value is  $L = 181 \mu\text{H}$  and an inductance value of  $200 \mu\text{H}$  was chosen for the converter.

**Capacitor:** The capacitor value is also determined based on the maximum capacity of the PV array. Considering the same operating conditions,  $I_o = 5.8\text{A}$ ,  $D = 0.65$ ,  $T_s = 25 \mu\text{s}$ . The output voltage ripple is selected to be 0.1% of its dc value (i.e.  $\Delta V_o = 0.012\text{V}$ ). The minimum capacitance value  $C$  is given by the following equation:

$$C = \frac{\Delta I_L T}{8 \Delta V_o} \quad (2)$$

Then  $C = (0.58 \times 25 \times 10^{-6}) / (8 \times 0.012) = 150 \mu\text{F}$ , and hence a  $220 \mu\text{F}$  capacitor is chosen for the design.

**Diode:** The choice of diode is a trade off between forward bias voltage, and switching speed. Diodes with low doping levels have fast recovery times but have higher forward bias voltage that will result in more power dissipation and loss. However, in our case a fast diode is required that can switch at high frequencies; if the diode is slow to react, the efficiency of the converter will drop. The best diode combining these features, that could be found, was the *STPS3045CPI* from SGS-THOMSON. It has a 0.57V of forward drop at a forward current of 15A.

### PIC SOFTWARE ALGORITHM

A PIC16F874 microcontroller is used to implement the Perturb and Observe (PAO) algorithm using an adaptive incremental step scheme. The program flow chart is shown in Figure 6. The program starts by initializing the A/D module and the PWM module. Then the battery state of charge is checked to prevent overcharge damage. If the battery is fully charged (e.g.  $> 13.8\text{V}$ ), then the PWM module is turned off for 1 second and the program runs A/D conversion again to measure the battery voltage. If the battery voltage is less than  $13.8\text{V}$  the program goes to a charging-tracking mode employing a Perturb and Observe algorithm.

### Charging-Tracking Mode

The microcontroller has a PWM output with having a duty cycle that is controllable by the associated software that implements the flow chart of the PAO adaptive algorithm shown in Figure 7. Two main paths are followed depending on whether the power  $P(n)$  has increased or decreased as compared to  $P(n-1)$ . Initially,  $P(0)$  is set to zero.

When the microcontroller is starting from rest, it starts hunting for the maximum power point by changing the duty cycle in a series of relatively large steps ( $\Delta = 32 / 255$ ). After each new step, it measures the voltage  $V_s$  and current  $I_s$  using the PIC built-in A/D channels, multiplies their digital representation, and compares the newly obtained power level with the former value.

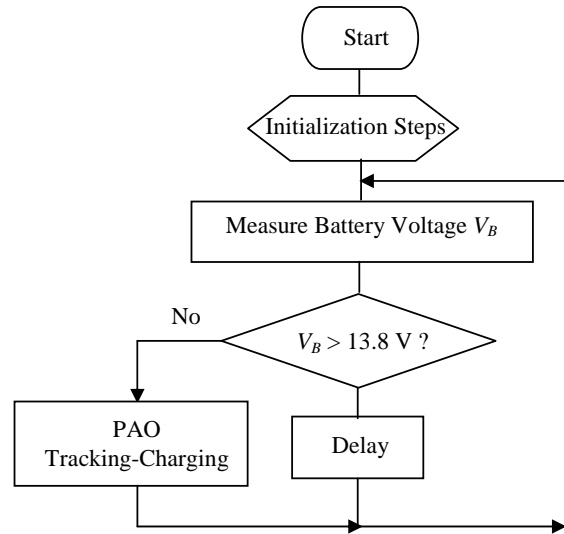


Figure 6. Program flow chart

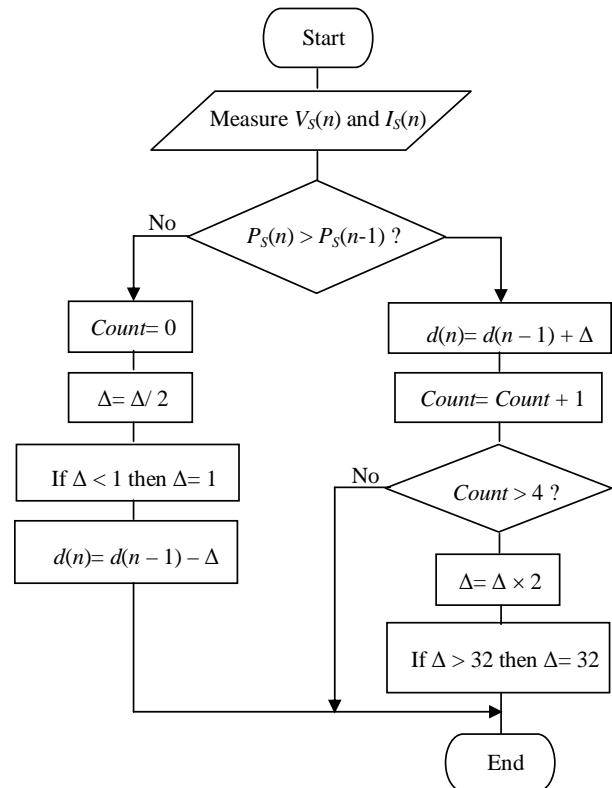


Figure 7. Adaptive PAO charging-tracking algorithm

Two cases may arise as a result of this comparison:

- If the newly obtained power is larger than the previously measured one, the microcontroller continues changing the duty cycle monotonically in the same direction, using the same step size ( $\Delta$ ).
- If the newly obtained power is lower than the previously measured one, the microcontroller reverses the direction of changing the duty cycle, and divides the step size  $\Delta$  by two.

Eventually, the microcontroller will reach a stage in its search for the maximum power point, where it jumps around the maximum power point in the smallest step (e.g.  $\Delta = 1/255$ ) as illustrated in Figure 8. The microcontroller should keep tracking, since the MPP is expected to vary due to changes of illumination and temperature depending on daytime, weather conditions, and shadow effects.

The tracking algorithm, just described, relates to the left path in Figure 7, which shows good performance for stable weather conditions with a tracking efficiency  $\xi_T$  reaching 95.6%. When a rapidly changing weather condition occurs, the PAO process will try to keep track of the new MPP, however, with a very small duty cycle increment reached so far. To enhance this tracking efficiency, when the power measured does not decrease for 4 consecutive steps the increment ( $\Delta$ ) is doubled. Without this adaptive portion, the PAO algorithm will become slower in tracking the MPP in case of rapidly varying weather conditions and the tracking efficiency  $\xi_T$  drops to less than 85%. The adaptive steps in tracking the MPP under varying weather conditions are illustrated in Figure 9 for a sudden increase in solar radiation.

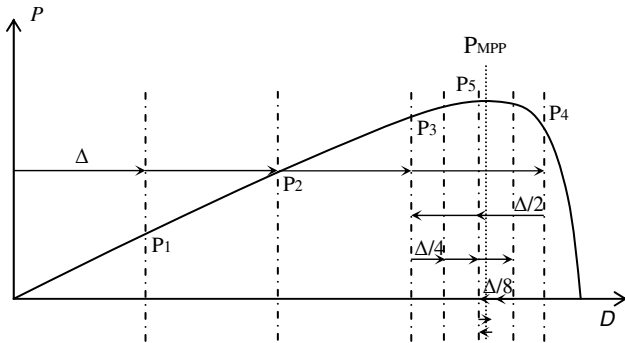


Figure 8. MPPT tracking using a variable step size

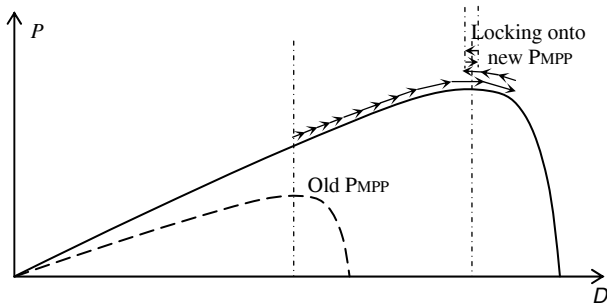


Figure 9. Tracking under varying weather conditions

## RESULTS

The MPPT hardware system with the adaptive PAO algorithm was tested under different weather conditions. First a variable load circuit was used to record the MPP data of the PV module prior to testing. For example, on the clear sunny day at noon in October 20, 2004, the MPP readings came to be:  $I_{MPP} = 4.13A$ ,  $V_{MPP} = 13.6V$  and  $P_{MPP} = 56.16W$ . The characteristic curves at mid-day are as shown in Figure 10.

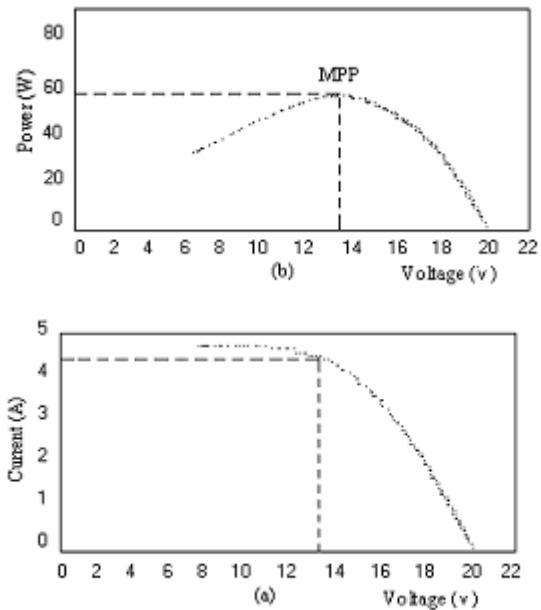


Figure 10. Characteristic curves: (a) I-V curve, (b) P-V curve

The system was tested on several days and the daily average readings obtained between 10:00 am and 5:00 pm are presented in Table 1 at the various mentioned dates. The value of the tracking efficiency reached a daily average efficiency of 95.6% and had an overall average value at 95% while the power electronics efficiency was about 80% on average. On a cold sunny day, the average power extracted from the PV module is greater than that of a hot sunny day, which is due to the fact that  $V_{oc}$  increases as the temperature decreases [7].

Table 1. MPP Daily Average Recorded Data 2004

Date	Weather condition	$P_{MPP}$ (W)	$P_S$ (W)	$P_B$ (W)	$\xi_T$ %	$\xi_{PE}$ %
29/4/04	Sunny day	49.9	47.5	38.0	95.0	80.0
30/4/04	Sunny day Few clouds	49.8	47.2	38.2	94.7	81.0
20/10/04	Hot Sunny day	54.7	52.3	42.0	95.6	80.3
23/10/04	Hot Sunny day	54.4	51.8	41.0	95.2	79.0
23/11/04	Cold Sunny day	62.7	59.7	48.9	95.2	82.0
24/11/04	Cold Sunny day	60.4	57.5	46.2	95.2	80.0
Average value					95	80

To measure the various sub-system efficiencies, the MPP data was first recorded and corresponding graph similar to that of Figure 10 is drawn. The MPPT hardware system was then set into action and a special Visual Basic (VB) program was developed to draw the voltage, current, and power versus time during tracking action and recorded the data shown in Figure 11 for October 20, 2004 around mid-day. The maximum power point is given as  $P_{MPP} = 54.7W$ , as shown in Table 1, and the average solar power, and voltage were  $P_S = 52.3W$  and  $V_S = 13V$ . Then the tracking efficiency is calculated as:  $\xi_{Tr} = P_S / P_{MPP} = 52.3 / 54.7 = 0.956$ . The power electronics efficiency was also measured:  $\xi_{PE} = P_B / P_S = 42 / 52.3 = 0.803$ , where  $P_B$  is the average power delivered to the battery.

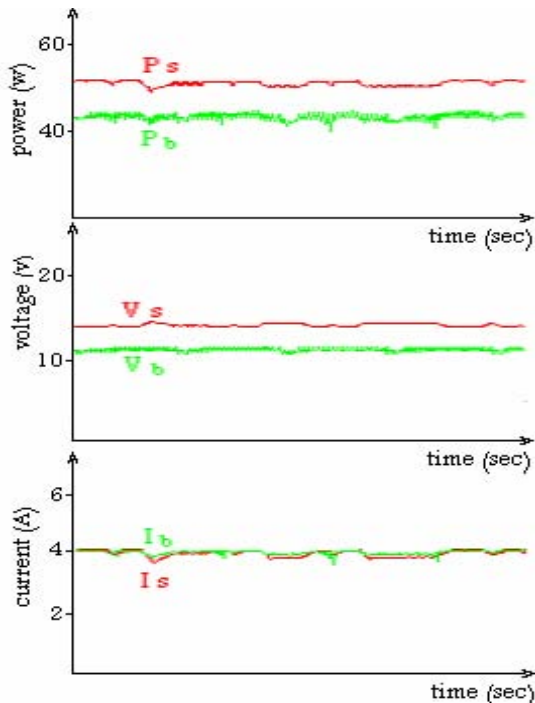


Figure 11. MPPT results at noon on October 20, 2004

Figure 12 shows how fast the adaptive PAO algorithm, implemented inside the controller, in tracking the MPP in case of changing weather conditions (varying solar radiation level due to the presence of clouds). Curve (a) represents the PV module varying MPP values due to weather conditions while curve (b) represents the power extracted from the PV module. The tracking efficiency  $\xi_T$  was 95% on average.

The power losses in the whole design system are estimated when operating in an MPP mode when the system was operating at 59.7W as measured on 23/11/04, shown in Table 1. The duty cycle  $D$  was set at 85%, the load current  $I_L$  was 5 A and the battery voltage was 12V. It was found that the total losses of the system amount to about 10.7W, which are estimated to be distributed as follows: inductor (0.84W), diodes (2.7W), MOSFETs (1.9W), transformer (0.46 W), and other circuitry (4.8W). The other circuitry includes the voltage and current sensing circuits, the microcontroller circuit, the printed copper track resistances and the copper wiring resistance.

The array utilization efficiency figure would improve as more arrays are stacked in series to supply a higher voltage level. Using the same simple technology presented in this paper, however, at the higher frequency of 80 kHz, it is estimated that the efficiency of the power electronics circuitry fed from 4 PV arrays charging a battery voltage of 48V would be at 92%. This will bring up the array utilization efficiency to  $0.90 \times 0.956 = 0.88$  on average.

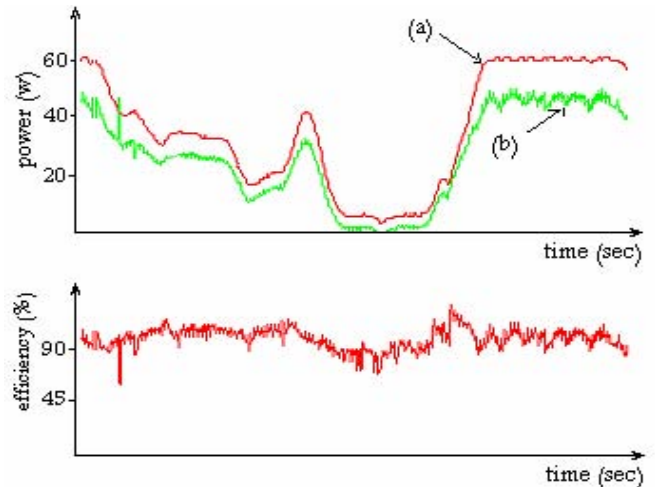


Figure 12. Tracking the MPP in case of varying solar radiation.

## CONCLUSIONS

This paper has presented a MPP tracking hardware system designed and tested around an adaptive PAO algorithm. The PAO algorithm is enhanced by allowing the size of the perturbation to increase or decrease adaptively based on the conditions of the search for the MPP. The system hardware consists of a PV module, an H-bridge transformer-coupled converter, a lead acid battery, and a control circuit that uses a PIC16F874 microcontroller. This algorithm showed good performance for stable weather conditions as well as rapidly changing weather condition with an average tracking efficiency of about 95%. The system was tested under real conditions and reported results showed that the daily average value for the tracking efficiency reached 95.6% with efficiency of the power electronics (PE) at 80.3%. This system has been developed with locally available hardware to validate the operation of the PAO adaptive algorithm. While still using the same simple technology, the efficiency can be significantly improved by increasing the frequency to 80 kHz and the voltage and power levels to 48V and 240 W, through using 4 similar PV arrays in series. The PE efficiency would increase to 92% yielding an overall efficiency of about 88%.

## REFERENCES

- [1] Hussein K.H., Muta I. , Hoshino T. , and Osakada M., "Maximum photovoltaic power tracking: an algorithm for rapidly changing atmospheric conditions", *IEE Proceeding on Generation Transmission and Distribution*, Vol. 142, No. 1, January 1995

- [2] Koutroulis E., Kalaitzakis K., and Voulgaris N. C., "Development of a Microcontroller-Based, Photovoltaic Maximum Power Point Tracking Control System", *IEEE Transactions on power electronics*, Vol. 16, No. 1, January 2001.
- [3] Lee D., Noh H. , Hyun D. , and Choy I., "An Improved MPPT Converter Using Current Compensation Method for Small Scaled PV-Applications", *Applied Power Electronics Conference and Exposition (APEC'03)*, Vol. 1, February 2003, pp. 540-545.
- [4] Yu G., Jung Y., Chol J., Choy I. , Song J., and Kim G., "A Novel Two-Mode MPPT Control Algorithm Based On Comparative Study of Existing Algorithms", *IEEE Photovoltaics Specialists Conference*, May 2002 pp. 1531-1534.
- [5] Masoum M. Dehbonei H., and Fuchs E., "Theoretical and Experimental Analyses of Photovoltaic Systems With Voltage- and Current-Based Maximum Power-Point Tracking", *IEEE Transactions Conversion*, Vol. 17, No.4, December 2002.
- [6] Sweigers W., and Enslin J., "An Integrated Maximum Power Point Tracker for Photovoltaic Panels", *Proceedings of IEEE International Symposium on Industrial Electronics. ISIE'98*, Vol. 1, July 1998, pp. 40-44.
- [7] Enslin J., Wolf M., Snyman D., and Swiegers W., "Integrated Photovoltaic Maximum Power Point Tracking Converter", *IEEE Transactions on Industrial Electronics*, Vol. 44, No.6, December 1997.
- [8] Hohm D., and Ropp M. "Comparative Study of Maximum Power Point Tracking Algorithms Using an Experimental Programmable Maximum Point Tracking Test Bed", *IEEE Photovoltaics Specialists Conference*, September 2000, pp.1699-1702.
- [9] Mohan N., Undeland T., Robbins W. *Power electronics: Converters, Applications and Design*, New Jersey: John Willey & Sons, 1989.

## BIOGRAPHIES

**Mohammed Serhan** is currently an instructor teaching at the Business and Computer University College in Lebanon. He received his Bachelor of Engineering in Electronics and Communications from Beirut Arab University (BAU) in 2002. He received his Master of Engineering in Electrical Engineering from the American University of Beirut in February 2005. His thesis work was to design, build and test a maximum power point tracking system. His research interests include power electronics and renewable energy where he is working on minimizing the size and cost of the MPPT system while increasing its efficiency and power handling capabilities.

**Sami H. Karaki** is professor of electrical engineering at the American University of Beirut (AUB), Lebanon. He joined AUB in 1991 and contributed to the development of its Electric Power Engineering program. From 1981 to 1990 he was with Kuwait Institute for Scientific Research, Kuwait where he contributed to two regionally leading projects on the power system interconnection of Arabic countries. He obtained his BE from AUB in 1975 and his Ph.D. from the University of Manchester Institute of Science and Technology, UK, in 1980. He is presently teaching courses in digital systems design, computer programming, power electronics, and power systems. His main research interests are in modeling of renewable energy systems, power system planning under competition, short-term load forecasting, and artificial intelligence applications in electric power systems.

**Lana R. Chaar** is a senior lecturer in the Department of Electrical and Computer Engineering at the American University of Beirut (AUB), Lebanon. She joined AUB in 1997. She taught electric circuits, digital systems, and electronics. She also supervised final year projects especially in the area of solar energy and power electronics. She obtained her BSEE in 1991, MSEE in 1993 and Ph. D. in 1996, all from the University of Minnesota (U of M), USA in the area of power electronics. Her main research interests are in the area of photovoltaic systems and their integration with utility grids.